ISSN 0023-1584, Kinetics and Catalysis, 2008, Vol. 49, No. 6, pp. 812–820. © Pleiades Publishing, Ltd., 2008.
Original Russian Text © A.V. Pashigreva, G.A. Bukhtiyarova, O.V. Klimov, G.S. Litvak, A.S. Noskov, 2008, published in Kinetika i Kataliz, 2008, Vol. 49, No. 6, pp. 855–864.

Influence of the Heat Treatment Conditions on the Activity of the $CoMo/Al_2O_3$ Catalyst for Deep Hydrodesulfurization of Diesel Fractions

A. V. Pashigreva, G. A. Bukhtiyarova, O. V. Klimov, G. S. Litvak, and A. S. Noskov

Boreskov Institute of Catalysis, Siberian Branch, Russian Academy of Sciences, Novosibirsk, 630090 Russia
e-mail: pav@catalysis.ru

Received March 28, 2008

Abstract—The effect of the heat treatment temperature on the sulfidation and activity of $CoMo/Al_2O_3$ catalysts designed for deep hydrodesulfurization of diesel fuel was studied. The catalysts were prepared using citric acid as a chelating ligand. The organic ligands present in the samples heat-treated at 110 and 220°C retard the decomposition of dimethyl disulfide and the formation of the sulfide phase but make the catalyst more active than the samples calcined at higher temperatures.

DOI: 10.1134/S0023158408060062

INTRODUCTION

New specifications for motor fuels have been introduced to meet the toughening requirements imposed on the concentration of noxious compounds in automotive exhaust. In Europe, diesel fuel with a sulfur content of at most 50 ppm has been used since 2005. From January 1, 2009, the sulfur content should not exceed 10 ppm [1]. In Russia the EURO-3 standard (350 ppm S) is coming into effect on January 1, 2009; EURO-4 (50 ppm S) take effect on January 1, 2013 [2].

In diesel fuel with a sulfur concentration of 300–500 ppm, the major S-containing components are low-reactive substituted alkyldibenzothiophenes with one or two alkyl groups in the positions nearest to the sulfur atom [3]. In order to reduce the sulfur content to 50 ppm, it is necessary to have catalysts active in the hydrodesulfurization of these stable compounds.

The conventional catalysts for hydrodesulfurization of diesel fractions are the $Co–Mo/Al_2O_3$ and $Ni–Mo/Al_2O_3$ sulfide systems. The modern views of the nature of the active phase of the Co(Ni)–Mo sulfide catalysts for hydrodesulfurization are based on the data obtained ex situ using a wide variety of physicochemical methods: high resolution transmission electron microscopy (HRTEM), X-ray photoelectron spectroscopy (XPS), the X-ray radial atomic distribution method, EXAFS, ^{57}Co Mössbauer spectroscopy, and others [4–8]. According to these views, the active components of the catalysts are fine MoS_2 particles with cobalt or nickel atoms localized in their lateral faces. These particles form the so-called Co(Ni)–Mo–S phase. Two types of this phase are described in the literature. The type I phase interacts more strongly with the support owing to Mo–Al–O bond formation and is sulfided to a lesser extent. By contrast, the type II Co(Ni)–Mo–S phase undergoes complete sulfidation and binds to the support surface only through van der Waals bonding [4–6, 9]. The specific activity of the type II phase (per Co atom) is considerably higher than that of the type I phase [4, 10]. In order to achieve high efficiency in the deep hydrodesulfurization of diesel fractions, the leading catalyst producers introduce high concentrations of the active component into the catalyst. On the alumina support surface, this component exists as the finely dispersed Co(Ni)–Mo–S sulfide phase of type II [11].

Supporting of active components from solutions containing chelating agents is an approach that makes it possible to form the active Co(Ni)–Mo–S phase dominated by type II on the support surface [12–27]. This approach was first used in [12], where nitrilotriacetic acid was introduced into the impregnating solution to enhance the activity of the $Co(Ni)–Mo/SiO_2$ catalysts. Later, many examples of use of other chelating ligands for the same purpose were reported. These include ethylenediaminetetraacetic and cyclohexadiaminetetraacetic acid [9, 13–21], citric acid [22–25], and thioglycolic acid [26, 27].

Chelating ligands favor the dispersion of active components on the support surface [13–16] and weaken the interaction of the active component (Mo) and promoter (Co) with the support, thus facilitating the formation of the active sulfide phase of the second type [10, 17–19]. In addition, in the presence of the chelating ligands, the sulfidation of Co (Ni) begins at a higher temperature simultaneously with the sulfidation of the Mo compounds [26, 27] or even after the formation of molybdenum sulfide [28–34]. This order of sulfidation decreases the probability of the formation of an individual Co phase and favors the location of Co on the lateral

faces of molybdenum sulfide particles and the formation of the active Co–Mo–S phase.

For Co–Mo/Al_2O_3 hydrodesulfurization catalysts prepared using chelating ligands, the influence of the heat treatment conditions on the formation of the active sulfide phase and on catalytic activity has not been studied in sufficient detail. An H_2S/H_2 gas mixture at atmospheric pressure has been used in the sulfidation of the catalysts in most studies, whereas in industry the catalysts are most often sulfided with a feedstock containing dimethyl disulfide and the process is carried out in the presence of hydrogen at a high pressure.

The purpose of this work is to study the influence of the heat treatment temperature on the sulfidation and activity of the CoMo/Al_2O_3 deep hydrodesulfurization catalysts prepared using citric acid as a chelating ligand. The catalysts were sulfided directly in the hydrodesulfurization reactor using a straight-run diesel fraction containing dimethyl disulfide as the sulfiding agent. Active phase formation was studied during the sulfidation of samples heat-treated under different conditions by comparing the variation of the amounts of dimethyl disulfide and the products of its decomposition in the diesel fuel and the variation of the methane and hydrogen sulfide concentrations in the hydrogen-containing gas at the outlet of the reactor.

EXPERIMENTAL

Catalyst Preparation

The catalyst was prepared by impregnating alumina support pellets with a solution containing Co and Mo complexes obtained by the simultaneous dissolution of ammonium paramolybdate $(NH_4)_6Mo_7O_{24} \cdot 4H_2O$ (analytical grade, Soviet Standard GOST 3765-64), cobalt acetate $Co(CH_3COO)_2 \cdot 4H_2O$ (high-purity grade, Soviet Standard GOST 5861-79), and citric acid $C_6H_8O_7 \cdot H_2O$ (reagent grade, Soviet Standard GOST 3652-69) [35]. The support was γ-Al_2O_3 shaped as rods 1.4 mm in diameter and 4.2–7.0 mm in length (produced at ZAO Promyshlennye Katalizatory, Ryazan, Russia). The specific surface area of the support was 285 m^2/g, the total pore volume was 0.82 cm^3/g, and the average pore diameter was 115 Å. The resulting wet catalyst dried at 110°C for 8–10 h was designated CoMo(110). The samples dried in a muffle furnace at 220, 300, and 400°C were designated CoMo(220), CoMo(300), and CoMo(400), respectively.

Testing of the Hydrodesulfurization Catalysts

The catalysts were sulfided, and their catalytic activity in the hydrodesulfurization of the diesel fraction was measured in a three-phase flow reactor with an inner diameter of 16 mm and an isothermal zone length of 300 mm. The raw materials and hydrogen were fed into the reactor from the top downwards. The diesel fraction was supplied using a Gilson-305 liquid chromatographic pump, and the hydrogen feed rate was controlled using a Bronkhorst automated flow controller. A well-known method for testing granulated catalysts in three-phase reactors was used in the experiments: 10 ml of the sample diluted with fine silicon carbide particles (0.25–0.50 mm size fraction) in a 1 : 1 ratio was loaded into the reactor [36–38]. In this case, the hydrodynamic characteristics of the reactor are governed by the packing of the small particles and the catalytic properties of the catalyst are estimated for particles of the same shape and size as those used in the industry [36].

The catalysts were sulfided directly in the reactor, using a straight-run diesel fraction additionally containing 0.6% sulfur as dimethyl disulfide. The commonly accepted procedure includes the following steps [39–41]:

(1) drying in a hydrogen flow at 120°C for 5 h,

(2) wetting of the catalyst with the feedstock and raising the hydrogen pressure in the reactor to 3.5 MPa,

(3) reducing the temperature to 230°C at a rate of 25 K/h,

(4) sulfidation at 230°C for 5 h (low-temperature stage),

(5) raising the reactor temperature to 340°C at a rate of 25 K/h, and

(6) sulfidation at 340°C for 8 h (high-temperature stage).

The sulfiding mixture was a light diesel fraction with a boiling end point of 340°C, which was fed at a volumetric flow rate of 2 h^{-1}. The H_2/diesel fraction ratio was 300. The dimethyl disulfide conversions in the presence of the catalysts were studied by monitoring the changes in the concentrations of dimethyl disulfide and the products of its decomposition in the sulfiding mixture and the concentrations of methane and hydrogen sulfide in the hydrogen-containing gas at the outlet of the reactor at all stages of sulfidation.

Catalytic properties were estimated from the residual sulfur content of the straight-run diesel fraction after hydrodesulfurization, which was carried out at 340°C, 3.5 MPa, a volumetric flow rate of 2 h^{-1}, and H_2/diesel fraction ratios of 300 and 200. The initial diesel fraction contained 11040 ppm sulfur, its density was 0.8550 g/cm^3, and its fractional composition was characterized by the following parameters: 10%, 241.4°C; 50%, 285.7°C; 90%, 340.1°C; boiling end point, 361°C. The residual sulfur content of the hydrogenizate was determined as the average for three samples taken 10, 11, and 12 h after the beginning the run under the given conditions.

Determination of the Concentration of Sulfur-Containing Compounds

An Agilent 6890N chromatograph equipped with an atomic emission detector (emission line from sulfur

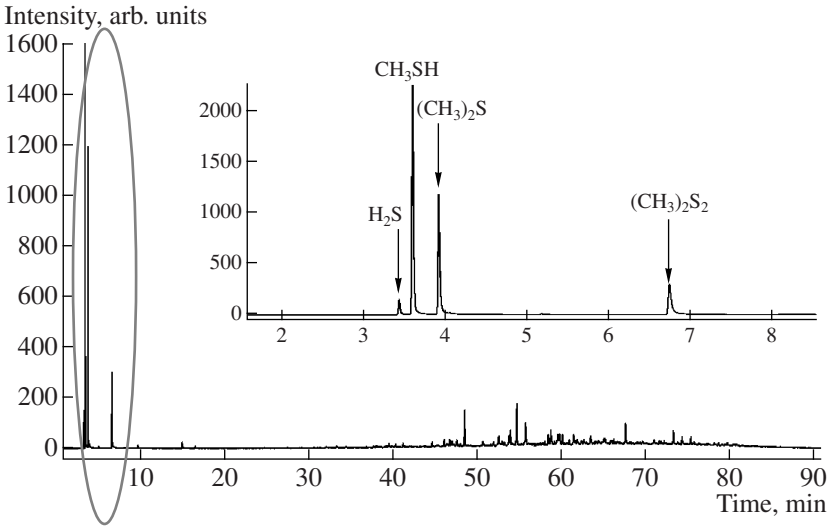

Fig. 1. Chromatogram of the hydrogenizate (S^{181}) after the contact between the sulfiding mixture and the CoMo(300) catalyst (temperature of 230°C, hydrogen pressure of 3.5 MPa, volumetric flow rate of 2 h^{-1}, H_2 : sulfiding mixture ratio of 300). The part of the chromatogram between 2 and 8 min is shown on an enlarged scale in the inset.

atoms at 181 nm, S^{181}) was used to determine the sulfur concentration in the initial diesel fuel and in the hydrogenizate and to identify and quantify the products of dimethyl disulfide decomposition in the sulfiding mixture. Diesel fuel components were separated on a 60-m-long HP-1MS capillary chromatographic column with an inner diameter of 0.32 mm and a film thickness of 0.25 μm, increasing the oven temperature from 40 to 240°C at a rate of 2 K/min and then to 260°C at a rate of 10 K/min.

The hydrogenizate was sampled for analysis at 30-min intervals. Quantitative analyses were carried out in terms of the areas of the S^{181} peaks at retention times of 3.43, 3.60, 3.90, and 6.75 min. These peaks were identified as being due to hydrogen sulfide, methylmercaptan, dimethyl sulfide, and dimethyl disulfide, respectively (Fig. 1).

The hydrogen sulfide and methane concentrations in the gas phase at the reactor outlet were determined with a thermal-conductivity detector using hydrogen as the carrier gas. The components were separated in a 2-m-long chromatographic column with an inner diameter of 2 mm packed with Chromosorb-104 at 120°C and a carrier gas flow rate of 30 ml/min. Analyses were made at 10-min intervals.

Characterization of the Catalysts by Physicochemical Methods

The main component (Co and Mo) contents of the oxide form of the catalyst were determined by the atomic absorption method. In the sample calcined at 550°C for 4 h, the Co concentration was 3.85 and the Mo concentration was 11.0 wt %.

Thermogravimetric analysis (TGA) and differential scanning calorimetry (DSC) of dried samples were carried out using a NETZSCH STA 449C-Jupiter instrument. The TGA and DSC curves were recorded between room temperature and 600°C in an air flow at a heating rate of 10 K/min. The sample (20 mg) was loaded into a corundum crucible. The reference sample was calcined alumina.

A Vario EL III element analyzer (ELEMENTAR Analysensysteme GmbH) was used to determine the carbon content of the samples in oxide form.

The S/Mo ratio in the samples after sulfidation and diesel fraction hydrodesulfurization tests was determined by X-ray fluorescence analysis on a VRA-30 analyzer with a Cr anode in the X-ray tube.

The catalyst was taken out of the reactor as follows. First, the reactor temperature was decreased to 40°C in the presence of the light diesel fraction (boiling end point of 340°C) and hydrogen, and then the diesel fraction was shut off and the flowing hydrogen was replaced with argon. Next, the pressure was dropped to atmospheric and the sample was cooled to room temperature. The sample was transferred under flowing argon into a vessel also filled with argon, and the vessel was sealed. Before analysis, the catalyst was washed with toluene and the solvent was distilled off in vacuo.

RESULTS

DTA Study of the Oxide Form of the Co–Mo Catalyst

The thermogravimetric (TG) and differential thermogravimetric (DTG) curves of the Co–Mo complex formed upon crystallization from the impregnating solution containing ammonium paramolybdate, cobalt acetate, and citric acid [42] are shown in Fig. 2.

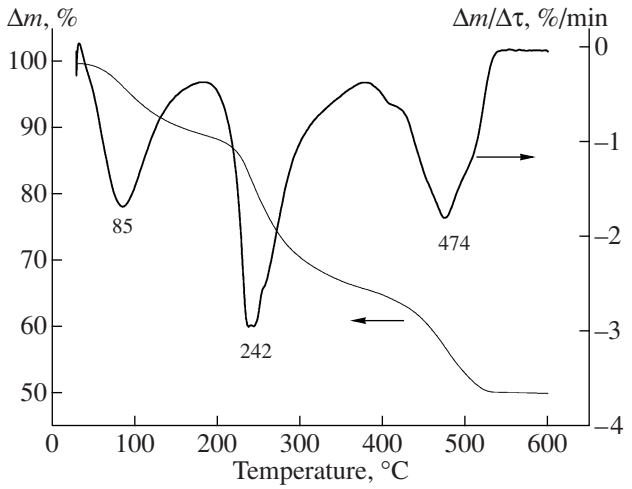

Fig. 2. TG and DTG curves of the Co-Mo complex formed upon crystallization from an impregnating solution containing ammonium paramolybdate, cobalt acetate, and citric acid [42].

Figure 3 presents the same curves for the Co–Mo samples heat-treated at different temperatures.

Three regions of rapid weight loss are observed on heating the Co–Mo complex, which are in the temperature ranges 50–150, 200–300, and 400–500°C (Fig. 2). This shape of the DTG curve is characteristic of the decomposition of citrate complexes [43–45]. The weight loss in the 50–150°C interval is due to the removal of adsorbed water, and at 200–300°C the citrate ligands decompose to form acetonedicarboxylate complexes [43] or oxycarbonate compounds [44]. The weight loss in the 400–500°C range, accompanied by a pronounced exotherm, is usually assigned to the oxidation of the remaining fragments of organic molecules [43–45].

The DTG curves of the catalysts heat-treated at 110, 220, 300, and 400°C indicate a rapid weight loss at 93–100°C, which is due to the removal of adsorbed water (Fig. 3). The peak at 245°C in the DTG curve of the CoMo(110) catalyst corresponds to a loss of 10.8% of the total sample weight and arises from the decomposition of the citrate ligands in the Co–Mo complex. This peak indicates that the complex is mainly localized on the support surface after the support is impregnated with a solution and then dried at 110°C. The peak corresponding to the decomposition of the citrate complex in the CoMo(220) sample is broader, its maximum is shifted to higher temperatures (302°C), and the weight loss is only 4.4%. This peak broadening suggests that the compounds undergoing decomposition are heterogeneous, and this heterogeneity can be a consequence of the partial and nonuniform decomposition of the complex during heat treatment at 220°C. The maximum weight loss for the CoMo(300) sample is observed at 448°C. It is likely that the citrate complexes decompose completely upon heat treatment at 300°C and carbon structures removable at a higher tempera-

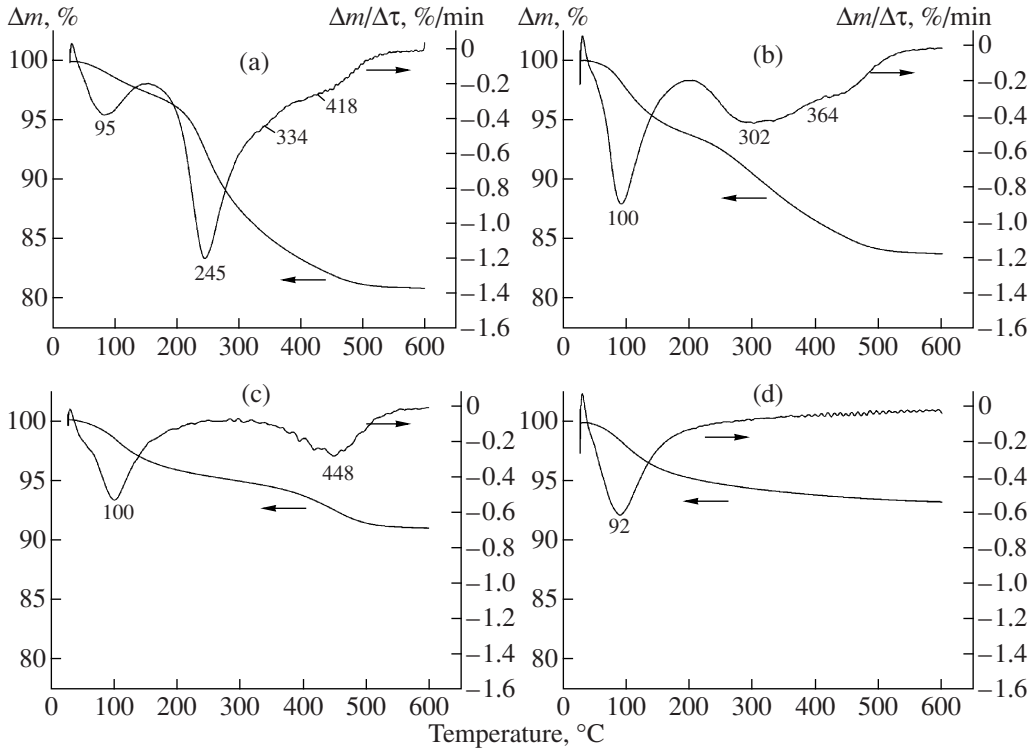

Fig. 3. TG and DTG curves of the Co–Mo catalyst samples subjected to heat treatment at (a) 110, (b) 220, (c) 300, and (d) 400°C.

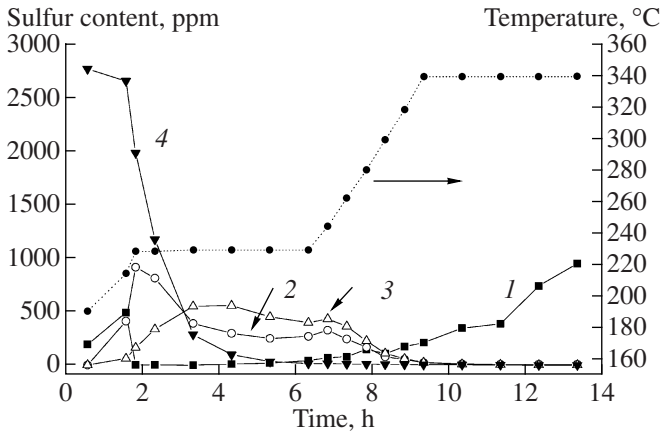

Fig. 4. Changes in the distribution of the products of dimethyl disulfide (DMDS) decomposition in the liquid phase during the sulfidation of the CoMo(300) catalyst: (*1*) H_2S, (*2*) CH_3SH, (*3*) $(CH_3)_2S$, and (*4*) DMDS.

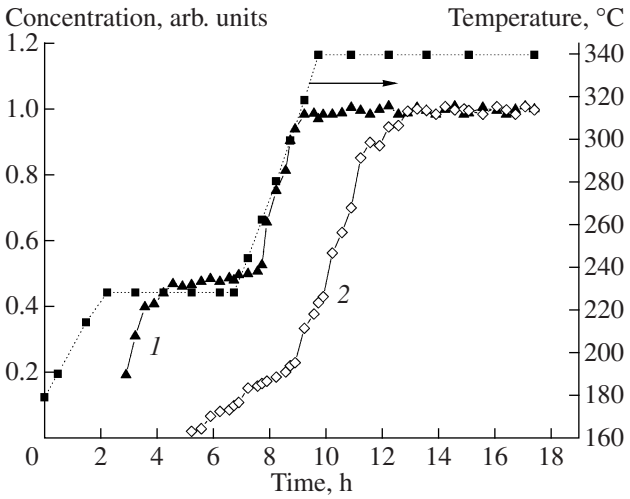

Fig. 5. Changes in the concentrations of (*1*) methane and (*2*) hydrogen sulfide in the gas phase during CoMo(300) catalyst sulfidation.

ture remain on the support surface. The DTG curve of the CoMo(400) sample contains only the peak corresponding to the loss of water, which means that heat treatment at 400°C results in the removal of all citrate ligands and their decomposition products.

These observations are quite consistent with the results of carbon determination on a Vario EL III element analyzer. The carbon content after heat treatment at 110, 220, 300, and 400°C was 5.78, 3.95, 1.79, and 0.05 wt %, respectively.

Sulfidation of the Catalysts

Let us analyze the variation dynamics of the concentrations of dimethyl disulfide and products of its conversion in the hydrogenizate and of the concentrations of hydrogen sulfide and methane in the gas phase at different temperatures and sulfidation durations using the CoMo(300) sample as an example.

The typical chromatogram of the sulfiding mixture after its contact with the catalyst is shown in Fig. 1. Figure 4 illustrates the changes in the concentrations of the light sulfur-containing products, namely, hydrogen sulfide, methylmercaptan, dimethyl sulfide, and dimethyl disulfide, during the sulfidation of the catalyst. Intermediate products of dimethyl disulfide decomposition appear in the hydrogenizate at 230°C, which are methylmercaptan CH_3SH and dimethyl sulfide $(CH_3)_2S$. As catalyst sulfidation at 230°C continues, the dimethyl disulfide content decreases and the dimethyl disulfide conversion reaches 100% at the end of the low-temperature stage. A methane peak appears in the chromatograms of the gas phase 1 h after the beginning of the low-temperature sulfidation stage. Its intensity gradually increases and becomes constant within 1 h (Fig. 5). Methane evolution into the gas phase indicates the decomposition of some portion of dimethyl disulfide with hydrogen sulfide formation. The H_2S peak appears much later than the CH_4 peak because, at the initial stage of the process, the resulting hydrogen sulfide is entirely consumed in the sulfidation of the catalyst.

At the next stage, as the sulfidation temperature increases from 230 to 340°C, the concentration of the intermediate products of dimethyl disulfide decomposition (methylmercaptan and dimethyl sulfide) in the sulfiding mixture begins to decrease and, above 300°C, no peaks of these compounds are observed in the chromatograms (Fig. 4). The methane and hydrogen sulfide contents of the gas phase increase as the temperature grows, and the CH_4 concentration becomes constant at ~300°C (Fig. 5). This indicates the complete decomposition of dimethyl disulfide and of more stable products of its conversion into methane and hydrogen sulfide and agrees well with the results of analysis of the sulfiding mixture.

The plots of the dimethyl disulfide content of the liquid phase versus the sulfidation temperature and duration for catalysts heat-treated at different temperatures are shown in Fig. 6. As can be seen, the dimethyl disulfide decomposition curves for the sulfidation of the CoMo(300) and CoMo(400) samples almost coincide. For these samples, dimethyl disulfide is almost absent in the sulfiding mixture at the end of the low-temperature stage. The intensive decomposition of dimethyl disulfide on the CoMo(100) and CoMo(200) catalysts begins later, especially on the former. In the presence of this catalyst, the dimethyl disulfide conversion in the 5th hour of the low-temperature sulfidation stage is about 70% and complete decomposition is achieved only at 340°C. The lower the catalyst heat treatment temperature, the later the dimethyl disulfide decomposition products (dimethyl sulfide and methylmercaptan) appear in the sulfiding mixture.

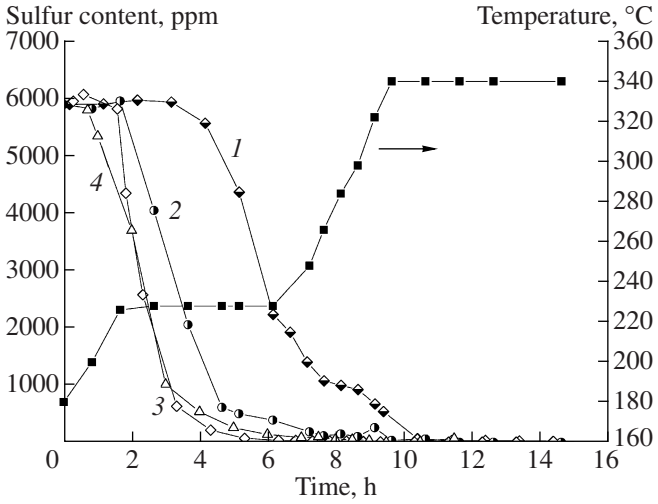

Fig. 6. Changes in the dimethyl disulfide concentration during the activation of the Co–Mo catalyst samples subjected to heat treatment at (*1*) 110, (*2*) 220, (*3*) 300, and (*4*) 400°C.

The changes in the methane and hydrogen sulfide concentrations in the gas phase at different sulfidation times for various samples are shown in Fig. 7. The higher the catalyst heat treatment temperature, the earlier methane appears in the gas phase. In this case, the methane evolution curves for CoMo(300) and CoMo(400) almost coincide.

For all catalyst samples, the methane concentration in the gas phase increases as the sulfidation temperature is raised from 230 to 340°C (Fig. 7a). For CoMo(300) and CoMo(400), the maximum CH_4 concentration is reached at ~300°C. At this temperature dimethyl disulfide and the intermediate products of its conversion decompose completely, which is in agreement with the results of analysis of the sulfur-containing compounds in the sulfiding mixture (Fig. 6). For the CoMo(220) sample, the maximum methane content of the gas phase is reached only at a sulfidation temperature of 340°C (Fig. 7a). An analysis of the variation of the hydrogen sulfide concentration in the gas phase (Fig. 7b) shows that, upon the sulfidation of all catalysts, hydrogen sulfide appears in the gas phase considerably later than methane. In the presence of CoMo(300) and CoMo(400), the hydrogen sulfide concentration increases noticeably at the stage of increasing the sulfidation temperature from 230 to 340°C, whereas, for the samples calcined at a lower temperature, this occurs only at the high-temperature stage (340°C).

Catalytic Properties

Residual sulfur content data for the hydrodesulfurization of the straight-run diesel fraction on Co–Mo catalysts heat-treated under different conditions are presented in the table. The CoMo(220) sample is most active. With the three other samples, the residual sulfur content of the hydrogenizate was higher.

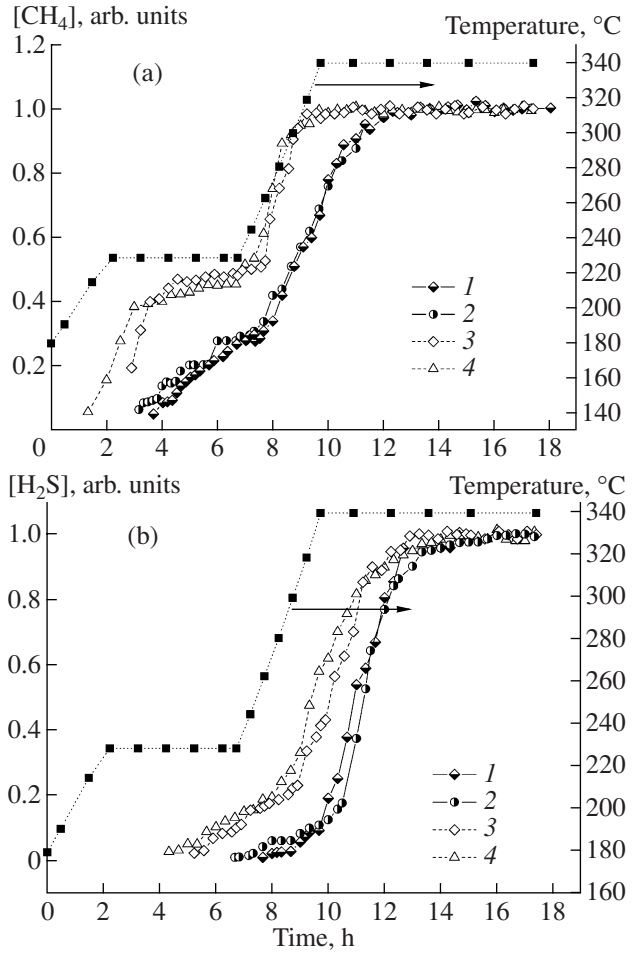

Fig. 7. Changes in the concentrations of (a) methane and (b) hydrogen sulfide in the gas phase during the sulfidation of the Co–Mo catalyst samples subjected to heat treatment at (*1*) 110, (*2*) 220, (*3*) 300, and (*4*) 400°C.

DISCUSSION

The dependence of catalytic activity on the heat treatment temperature for the Co–Mo/Al_2O_3 catalysts prepared using citric acid as the chelating ligand can be explained on the basis of the DTA data concerning the composition of the oxide precursors and on the specific features of the sulfidation of the samples by diesel fuel containing dimethyl disulfide.

Sulfidation is the most important stage of preparation of the hydrodesulfurization catalysts, and it determines the structure of the active component and catalytic activity. The modern views of the mechanism of sulfidation of Mo-containing catalysts are based on the studies of this process on calcined catalysts being treated with an H_2S/H_2 mixture. The temperature-programmed reaction (in this case, sulfidation) method [46–48], EXAFS [49–51], and Raman spectroscopy [52, 53] are used for this purpose. Independent authors believe that the formation of MoS_2 particles on the support surface proceeds through the intermediate forma-

Residual sulfur content of the straight-run diesel fraction after its hydrodesulfurization on various samples of the Co–Mo catalyst

H_2/diesel fraction molar ratio	Residual sulfur content, ppm			
	CoMo(110)	CoMo(220)	CoMo(300)	CoMo(400)
300	69	41	75	104
200	86	70	98	150

Note: Hydrodesulfurization temperature, 340°C; hydrogen pressure, 3.5 MPa; volumetric flow rate, 2 h^{-1}.

tion of molybdenum oxysulfides [46–48, 51–53] or MoS_3 [32, 48, 50], which are amorphous compounds whose structures have not been determined conclusively. These intermediate compounds begin to form even at room temperature due to the fast exchange of O and S atoms between the reactive oxygen of molybdenum oxide and sulfur of hydrogen sulfide [46, 47, 53]. In the presence of hydrogen, as the temperature is increased, their reduction yielding MoS_2 begins, which usually occurs above 300°C. However, above 300°C the reduction reaction begins to compete with the sulfidation reaction and MoO_2 can be formed along with MoS_2 on the catalyst surface. Under these conditions, the sulfidation of MoO_2 is greatly retarded [39]. Therefore, it is necessary that the formation of intermediate oxysulfide or sulfide compounds should occur at temperatures not higher than 300°C [32, 39].

The catalyst is sulfided by dimethyl disulfide due to the interaction of the oxide precursors with H_2S or methylmercaptan, which result from dimethyl disulfide decomposition. The experimental data on dimethyl disulfide decomposition on the CoMo(300) sample (Figs. 4, 5) are consistent with the known dimethyl disulfide conversion mechanism consisting of several steps [39].

Methylmercaptan is formed at the low-temperature sulfidation stage due to dimethyl disulfide hydrogenolysis:

$$CH_3–S–S–CH_3 + H_2 \longrightarrow 2CH_3SH. \quad (I)$$

The condensation of the resulting methylmercaptan in this step yields dimethyl sulfide:

$$2CH_3SH \longrightarrow CH_3–S–CH_3 + H_2S. \quad (II)$$

The products of methanemercaptan hydrogenolysis on the catalyst surface are methane and hydrogen sulfide:

$$CH_3SH + H_2 \longrightarrow CH_4 + H_2S. \quad (III)$$

Dimethyl disulfide can also decompose to hydrogen sulfide and methane:

$$CH_3–S–S–CH_3 + 3H_2 \longrightarrow 2CH_4 + 2H_2S. \quad (IV)$$

However, the contribution from this reaction is small at low temperatures [39].

The resulting hydrogen sulfide and methylmercaptan react with the oxide precursors, gradually yielding a sulfide phase on the surface. This phase, in turn, begins to initiate the decomposition of dimethyl disulfide and methylmercaptan. Methane appears in the gas phase soon after the temperature of the first (low-temperature) sulfidation stage is achieved. This moment can be considered as the beginning of active dimethyl disulfide decomposition. Hydrogen sulfide participates in the formation of the active sulfide component and appears in the gas phase in smaller amounts and much later, after sulfiding the major part of the active metals.

Thus, the mechanism suggested above for Co–Mo catalysts prepared by the standard method is indeed observed for the CoMo(300) and CoMo(400) catalysts. Dimethyl disulfide decomposes to methylmercaptan already at 130°C, and at 230°C dimethyl disulfide hydrogenolysis occurs actively to evolve hydrogen sulfide and methane [39]. The calcination of the samples above 300°C results in the destruction of the complex, due to which the Co and Mo atoms can interact with the sulfiding agent at low temperatures.

A comparative analysis of the changes in the concentrations of dimethyl disulfide and the products of its conversion in the presence of the Co–Mo catalysts heat-treated at different temperatures shows that dimethyl disulfide conversion on these samples proceeds via the same mechanism. However, the lower the temperature at which the oxide precursor of the hydrodesulfurization catalyst is heat-treated, the later the decomposition of the sulfurizing agent to methylmercaptan and hydrogen sulfide and, accordingly, the sulfidation of the sample begin.

In our opinion, this effect can be explained as follows. According to DTA data, the oxide precursors of the active component of the sample dried at 110°C almost completely retain the structure of the initial Co–Mo complex with the citrate ligands. This structure decomposes partially as the heat treatment temperature is increased to 220°C, but the Co and Mo atoms stay in the environment of carbon intermediates, which stabilize them on the support surface.

The sulfidation of the CoMo(110) and CoMo(220) samples is slower than the sulfidation of the CoMo(300) and CoMo(400) samples due to the stabilizing effect of the citrate ligands. Therefore, the Co and Mo atoms in the catalysts calcined at temperatures not higher than 220°C are components of the stable compounds. At the stage of low-temperature activation at 230°C, the decomposition of the carboxylate ligands of the starting complex begins and the Co and Mo compounds capable of interacting with the sulfiding agents gradually appear on the surface. The continuous increase in the methane concentration in the gas phase during the sulfidation of such catalysts (Fig. 7) indicates that the active sites involved in the hydrogenolysis

of dimethyl disulfide continue to form throughout the stage of temperature increase.

The formation of the active component retaining the structure of the initial complex takes place simultaneously with the decomposition of the citrate complexes, providing the conditions necessary for a more intimate interaction between the atoms of the active component (Mo) and the promoter (Co) at the sulfidation stage. This is why the CoMo(110) and CoMo(220) samples are more active than CoMo(300) and CoMo(400). Our results are in agreement with the view that, for preparing an active catalyst, sulfidation should be carried out under conditions such that the Co and Mo atoms are in close contact, for example, in one complex [27, 49]. If the structure of the initial complex persists at the heat treatment stage, the conversion of the surface oxide compounds into sulfide form proceeds slowly, and the lower activity of the CoMo(110) sample as compared to CoMo(220) can be explained by the insufficient saturation of the active component particles with sulfur during the low-temperature activation stage.

Perhaps the sulfidation of the active component of the catalyst remains incomplete in this case. This assumption is confirmed by the results of special experiments, according to which an increase in the sulfidation duration for the CoMo(110) sample reduces the residual sulfur content of the hydrogenizate to values comparable with the residual sulfur content achieved with the CoMo(220) catalyst. The finding that the catalysts whose active components retain their ligand environment after heat treatment are difficult to sulfidize provides an explanation for published data according to which calcined catalysts prepared using chelating ligands are more active [54, 55]. It is likely that inefficient sulfidation, not inappropriate heat treatment conditions, is the cause of the decrease in the catalytic activity.

Our experimental data confirm the view that heat treatment should be limited to the drying stage in order to achieve the maximum activity of the catalysts prepared using the chelating ligands [12, 23, 34, 56, 57]. The heat treatment temperature may differ from the standard drying temperature (110°C), but the complex compound (precursor of the active component) should survive on the surface. A comparative analysis of the sulfidation of samples heat-treated at different temperatures shows that, if the structure of the initial complex is retained at the heat treatment stage, the conversion of the surface oxide compounds into the sulfide form is slow. Therefore, for a high activity of the catalysts prepared using the chelating ligands, they should be sulfided in such a way that a sufficient amount of hydrogen sulfide is present at the low-temperature stage.

REFERENCES

1. Eijsbouts, S., Battiston, A.A., and van Leerdam, G.C., *Catal. Today*, 2008, vol. 130, p. 361.
2. Levinbuk, M.I., Netesanov, S.D., Lebedev, A.A., et al., *Neftekhimiya*, 2007, vol. 74, p. 252 [*Pet. Chem.* (Engl. Transl.), vol. 74, p. 230].
3. Bej, S.K., Maity, S.K., and Turaga, U.T., *Energy Fuels*, 2004, vol. 18, p. 1227.
4. Topsøe, H., Clausen, B.S., Massoth, F.E., Anderson, J.R., and Boudart, M., *Catalysis: Science and Technology,* Berlin: Springer, 1996, vol. 11.
5. Prins, R., *Handbook of Heterogeneous Catalysis*, Berlin: VCH, 1997, vol. 4.
6. Bouwens, S.M.A.M., Vanzon, F.B.M., Vandijk, M.P., Vanderkraan, A.M., de Beer, V.H.J., Vanveen, J.A.R., and Koningsberger, D.C., *J. Catal.*, 1994, vol. 146, p. 375.
7. Lauritsen, J.V., Kibsgaard, J., Olesen, G.H., Moses, P.G., Hinnemann, B., Helveg, S., Norskov, J.K., Clausen, B.S., Topsøe, H., Lgsgaard, E., and Besenbacher, F., *J. Catal.*, 2007, vol. 249, p. 218.
8. Startsev, A.N., *Sul'fidnye katalizatory: sintez, struktura, svoistva* (Sulfide Catalysts: Synthesis, Structure, and Properties), Novosibirsk: Geo, 2007.
9. Van Veen, J.A.R., Colijn, H.A., Hendrics, P.A.J.M., and van Welsenes, A.J., *Fuel Process. Technol.*, 1993, vol. 35, p. 137.
10. Van Veen, J.A.R., Gerkema, E., van der Kraan, A.M., Hendrics, P.A.J.M., and Beens, H., *J. Catal.*, 1992, vol. 133, p. 112.
11. Topsøe, H., *Appl. Catal., A*, 2007, vol. 322, p. 3.
12. Patent EP 0181035, 1986.
13. Blanchard, P., Lamonier, C., Griboval, A., and Payen, E., *Appl. Catal., A*, 2007, vol. 322, p. 33.
14. Inamura, K., Ushikawa, K., and Matsuda, S., *Appl. Surf. Sci.*, 1997, vol. 121/122, p. 468.
15. Shimizu, T., Hiroshima, K., Mochizuki, T., Honma, T., and Yamada, M., *Catal. Today*, 1998, vol. 45, p. 271.
16. Van Dillen, A.J., Terorde, R.J.A.M., Lensveld, D.J., Geus, J.W., and de Jong, K.P., *J. Catal.*, 2003, vol. 216, p. 257.
17. Sun, M., Nicosia, D., and Prins, R., *Catal. Today*, 2003, vol. 86, p. 173.
18. Hensen, E.J.M., de Beer, V.H.J., van Veen, J.A.R., and van Santen, R.A., *Catal. Lett.*, 2002, vol. 84, p. 59.
19. Al-Dalama, K. and Stanislaus, A., *Energy Fuels*, 2006, vol. 20, p. 1777.
20. Sundaramurthy, V., Dalai, A.K., and Adjaye, J., *Catal. Lett.*, 2005, vol. 102, p. 299.
21. Trejo, F., Rana, M.S., and Ancheyta, J., *Catal. Today*, 2008, vol. 130, p. 327.
22. Yoshimura, Y., Matsubayashi, N., Sato, T., Shimada, H., and Nishijima, A., *Appl. Catal., A*, 1991, vol. 79, p. 145.
23. Fujikawa, T., Kimura, H., Kiriyama, K., and Hagiwara, K., *Catal. Today*, 2006, vol. 111, p. 188.
24. Fujikawa, T., *Catal. Surv. Asia*, 2006, vol. 10, p. 89.
25. Pereira, L.G., Araujo, A.S., Souza, M.J.B., et al., *Mater. Lett.*, 2006, vol. 60, p. 2638.
26. Frizi, N., Blanchard, P., Payen, E., Baranek, P., Lancelot, C., Pebeilleau, M., Dupuy, C., and Dath, J.P., *Catal. Today*, 2008, vol. 130, p. 32.

27. Frizi, N., Blanchard, P., Payen, E., Baranek, P., Lancelot, C., Pebeilleau, M., Dupuy, C., and Dath, J.P., *Catal. Today*, 2008, vol. 130, p. 272.
28. De Jong, A.M., de Beer, V.H.J., van Veen, J.A.R., and Niemantsverdriert, J.W., *J. Phys. Chem.*, 1996, vol. 100, p. 17722.
29. Ohta, Y., Shimizu, T., Honma, T., and Yamada, M., *Stud. Surf. Sci. Catal.*, 1999, vol. 127, p. 161.
30. Hiroshima, K., Mochizuki, T., Honma, T., Shimizu, T., and Yamada, M., *Appl. Surf. Sci.*, 1997, vol. 121/122, p. 433.
31. Lelias, M.A., van Gestel, J., Mauge, F., and van Veen, J.A.R., *Catal. Today*, 2008, vol. 130, p. 109.
32. Medici, L. and Prins, R., *J. Catal.*, 1996, vol. 163, p. 38.
33. Coulier, L., de Beer, V.H.J., van Veen, J.A.R., and Niemantsverdriet, J.W., *Top. Catal.*, 2000, vol. 13, p. 99.
34. Cattaneo, R., Weber, T., Shido, T., and Prins, R., *J. Catal.*, 2000, vol. 191, p. 225.
35. RF Patent 2312886, 2007.
36. Bej, S.K., *Energy Fuels*, 2002, vol. 16, p. 774.
37. Sertic-Bionda, K., Gomzi, Z., and Saric, T., *Chem. Eng. J.*, 2005, vol. 106, p. 105.
38. http://www.cperi-solutions.gr/hbusite/services.htm
39. Texier, S., Berhault, G., Perot, G., Harle, V., and Diehl, F., *J. Catal.*, 2004, vol. 223, p. 404.
40. Marroquin, G., Ancheyta, J., and Diaz, J.A.I., *Catal. Today*, 2004, vol. 98, p. 75.
41. Eijsbouts, S., van den Oetelaar L.C.A., and van Puijenbroek, R.R., *J. Catal.*, 2005, vol. 229, p. 352.
42. Klimov, O.V., Pashigreva, A.V., Fedotov, M.A., Kochubey, D.I., Chesalov, Yu.A., Bukhtiyarova, G.A., and Noskov, A.S., *Catal. Today* (in press).
43. Gajbhiye, N.S. and Balaji, G., *Thermochim. Acta*, 2002, vol. 385, p. 143.
44. Rajendran, M. and Rao, M.S., *J. Mater. Res.*, 1994, vol. 9, p. 2277.
45. Bocher, L., Aguirre, M.H., Trottmann, M., Logvinovich, D., Hug, P., and Weidenkaff, A., *Thermochim. Acta*, 2007, vol. 457, p. 11.
46. Sheffer, B., Mangus, P.J., and Moulijn, J.A., *J. Catal.*, 1990, vol. 121, p. 18.
47. Arnoldy, P., van den Heijkant J.A.M., de Bok, G.D., and Moulijn, J.A, *J. Catal.*, 1985, vol. 92, p. 35.
48. Iwamoto, R., Inamura, K., Nozaki, T., and Iino, A., *Appl. Catal., A*, 1997, vol. 163, p. 217.
49. Nicosia, D. and Prins, R., *J. Catal.*, 2005, vol. 231, p. 259.
50. Leliveld, R.G., van Dillen, A.J., Geus, J.W., and Koningsberger, D.C., *J. Catal.*, 1997, vol. 171, p. 115.
51. Chiu, N.-S., Bauer, S.H., and Johnson, M.F.L., *J. Catal.*, 1986, vol. 98, p. 32.
52. Schrader, G.L. and Cheng, C.P., *J. Catal.*, 1983, vol. 80, p. 369.
53. Payen, E., Kasztelan, S., Houssenbay, S., Szymanski, R., and Grimblot, J., *J. Phys. Chem.*, 1989, vol. 93, p. 6501.
54. Okamoto, Y., Ishihara, S., Kawano, M., Satoh, M., and Kubota, T., *J. Catal.*, 2003, vol. 217, p. 12.
55. Trejo, F., Rana, M.S., and Ancheyta, J., *Catal. Today*, 2008, vol. 130, p. 327.
56. Fujikawa, T., Kato, M., Kimura, H., Kiriyama, K., Hashimoto, M., and Nakajima, N., *J. Japan Petrol. Inst.*, 2005, vol. 48, p. 106.
57. Bouwens, S.M.A.M., van Zon, F.B.M., and van Dijk, M.P., *J. Catal.*, 1994, vol. 146, p. 375.